Thermodynamical mode selection rule observed in thermoacoustic oscillations

EUROPHYSICS LETTERS 1 November 2002

Europhys. Lett., **60** (3), pp. 363–368 (2002)

Thermodynamical mode selection rule observed in thermoacoustic oscillations

T. Biwa[1], Y. Ueda[1], T. Yazaki[2] and U. Mizutani[1]

[1] *Department of Crystalline Materials Science, Nagoya University Furo-cho, Chikusa-ku, Nagoya 464-8603, Japan*

[2] *Department of Physics, Aichi University of Education Kariya, 448-8542, Japan*

(received 7 January 2002; accepted in final form 12 August 2002)

PACS. 43.35.Ud – Thermoacoustics, high temperature acoustics, photoacoustic effect.
PACS. 05.70.Ln – Nonequilibrium and irreversible thermodynamics.

Abstract. – A gas column in a tube with a temperature gradient spontaneously begins to oscillate when it is driven away from equilibrium. We observed a transition from the standing- to the traveling-acoustic-wave modes through a quasiperiodic state using a looped tube attached to a resonator. Through the measurements of entropy flow, we experimentally propose a thermodynamical mode selection rule, which acts as a guiding principle for a sequence of unstable modes appearing in nonequilibrium systems.

A gas column in a tube equipped with a *stack* of plates and adjacent heat exchangers spontaneously begins to oscillate when it is driven away from equilibrium by externally supplied heat power. Such a thermoacoustic oscillation constitutes one of the dissipative structures in nonequilibrium systems [1], and distinctively functions as a heat engine converting the *heat flow* Q into the *acoustic work flow* I within the stack [2–5]. Experimental studies on thermoacoustic engines so far concentrated on standing-wave engines equipped with a *resonator* [6–8], where a standing wave contributes to the mutual energy conversion between Q and I through the irreversible thermodynamical process. More recently, however, traveling-wave engines have been constructed by using a *looped tube* [9, 10], where a traveling wave is responsible for the energy conversion through the reversible thermodynamical process.

In this experiment, we have built a thermoacoustic engine by combining a looped tube and a resonator. In that way both the standing- and traveling-wave modes having different oscillating frequencies can be excited. In order to shed a new light on dissipative structures from the thermodynamical point of view, we investigate an increase in the *entropy flow* S along the stack associated with the thermoacoustic oscillation as well as that without the oscillation by measuring energy flows in the present thermoacoustic engine. In this letter, we here for the first time propose the existence of a mode selection rule according to which a mode having a minimum increase in entropy flow is selected when more than one nonequilibrium mode is possible [11]. This rule would play a crucial role in the thermodynamical interpretation of the transition sequences observed in nonlinear dissipative systems [12, 13].

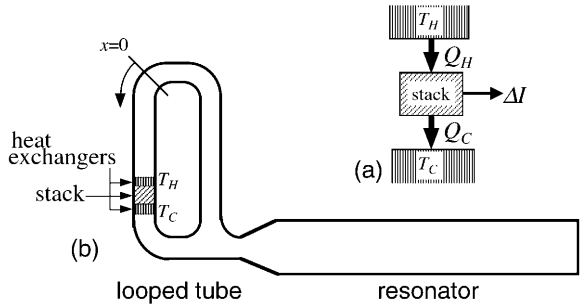

Fig. 1 – Schematic diagram of (a) the heart of a thermoacoustic prime mover and (b) the experimental setup consisting of a resonator and a looped tube containing the assembly shown in (a) inside. The origin of the coordinate x normalized with respect to the total length of the looped tube is taken at the position where the pressure amplitude for the standing-wave mode takes its maximum in the looped tube. The center of a stack is located at $x = 0.32$ in this scale.

Figure 1(a) schematically illustrates a stack and two heat exchangers with temperatures $T_{\rm H}$ and $T_{\rm C}$, all of which are contained in a tube filled with a working fluid. Axial heat flow $Q_{\rm H}$, a nonequilibrium parameter in this experiment, is supplied to the stack through the hot heat exchanger. When $Q_{\rm H}$ exceeds some critical value $Q_{\rm cri}$, a gas column in the tube spontaneously begins to oscillate. Under the steady-state operation of the engine, the heat flow $Q_{\rm H}$ entering from the hot end of the stack is partly converted to the output power ΔI within the stack, and the rest, $Q_{\rm C}$, is removed from the cold end of the stack. The energy conservation law assures the relation

$$Q_{\rm H} = Q_{\rm C} + \Delta I. \tag{1}$$

We focus on the entropy flow S [14] instead of entropy being a state function, since the engine is in a nonequilibrium steady state. The entropy flow S is defined as $S = Q/T$ by using the heat flow Q passing through the cross-section at temperature T, and hence those at the hot and cold ends of the stack are given as $S_{\rm H} = Q_{\rm H}/T_{\rm H}$ and $S_{\rm C} = Q_{\rm C}/T_{\rm C}$, respectively. Consequently, the increase in the entropy flow ΔS through the stack is given by $\Delta S = Q_{\rm C}/T_{\rm C} - Q_{\rm H}/T_{\rm H}$. When the oscillation is absent, the relation $Q_{\rm H} = Q_{\rm C}$ holds. Therefore, ΔS is given by

$$\Delta S = \left(\frac{1}{T_{\rm C}} - \frac{1}{T_{\rm H}} \right) \cdot Q_{\rm H} > 0. \tag{2}$$

On the other hand, when the oscillation is self-sustained, the output power ΔI must be finite and hence ΔS is obtained as

$$\Delta S = \left(\frac{1}{T_{\rm C}} - \frac{1}{T_{\rm H}} \right) \cdot Q_{\rm H} - \frac{\Delta I}{T_{\rm C}}. \tag{3}$$

If the energy conversion proceeds through the reversible process, ΔS should be zero and then the engine efficiency $\Delta I/Q_{\rm H}$ is given by Carnot's efficiency ($= 1 - T_{\rm C}/T_{\rm H}$). It is of vital importance to note here that we can experimentally determine ΔS as a function of the nonequilibrium parameter $Q_{\rm H}$ through the measurements of ΔI, $T_{\rm H}$ and $T_{\rm C}$, by using eq. (3).

Figure 1(b) shows the schematic illustration of the present thermoacoustic engine consisting of a looped tube and a resonator. The total lengths of the loop and the resonator are 1.23 m and 1.00 m, respectively. The looped tube is made of Pyrex glass with its internal diameter of 40 mm, and the resonator is made of stainless steel and its internal diameter is 73 mm. A

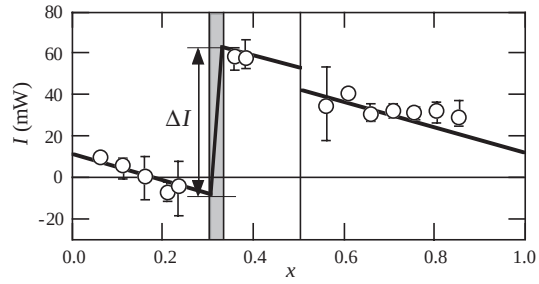

Fig. 2 – Axial distribution of the work flow measured when $Q_{\mathrm{H}} = 86\,\mathrm{W}$. A shaded region and a vertical line represent a stack and the position connecting the looped tube with a resonator, respectively. The output power ΔI is shown as the difference in the work flow between hot and cold ends of the stack. A negative slope of I in regions except for the stack represents the dissipated power per unit length in the looped tube. The power supplied to the resonator is represented by the discontinuous drop of I at $x = 0.5$.

ceramic stack, having many square channels with their sides of 0.93 mm, is located in the loop together with hot and cold heat exchangers. A sheathed thermocouple was inserted into the hot heat exchanger to monitor its temperature T_{H}. An electrical heater was wound around the hot heat exchanger to feed the heat flow Q_{H} to the stack, and the cooling water pipe was wound around the cold heat exchanger to keep its temperature T_{C} at room temperature. Air at one bar atmospheric pressure was used as the working fluid. While the value of Q_{cri} is found to depend on the position of the assembly shown in fig. 1(a), the value of $Q_{\mathrm{cri}} = 60\,\mathrm{W}$ was obtained when the setup with the geometry shown in fig. 1(b) was employed [15].

The fundamental frequency of the acoustic oscillation induced above Q_{cri} is 100 Hz. We simultaneously measured both the pressure and velocity of the oscillating gas (see [8] in more details) along the axial coordinate x directed anticlockwise in the loop, by using pressure transducers and laser Doppler velocimeter, respectively, and determined the work flow from the equation

$$I = A\overline{P \cdot U} = \frac{1}{2} Apu \cos \Phi, \tag{4}$$

where a bar indicates a time average and A is the cross-sectional area of the gas passage, p is the amplitude of the pressure P, u is that of the cross-sectional mean velocity U and Φ is the phase lead of U relative to P.

The axial distribution of the work flow I measured when $Q_{\mathrm{H}} = 86\,\mathrm{W}$, just above Q_{cri}, is shown in fig. 2, where the flow direction is indicated by its sign. The slope of I is always negative in all the regions outside the stack, showing the dissipation of the acoustic power on the tube wall. On the other hand, a positive slope does exist in the stack, indicating the production of the acoustic power emitting from the stack. Now we see that the output power ΔI of the present engine is given by a total increase of I, which can be read off from the graph as the difference in I between the hot and cold ends of the stack to be about 70 mW. It should be mentioned here that I crosses zero in the stack. This means that Φ in eq. (4) is $\pi/2$ and that the energy conversion is achieved by a standing wave. In other words, the present engine begins to oscillate in a standing-wave mode [16]. In a traveling-wave engine, the work flow I runs from T_{C} to T_{H} without changing the flow direction within the stack [10]. Therefore, we can determine not only the magnitude of the output power ΔI, but also whether the induced oscillation is the standing- or traveling-wave mode, through the work flow measurements.

Figures 3(a) and (b) show ΔI and T_{H} as a function of Q_{H}, respectively. The variation

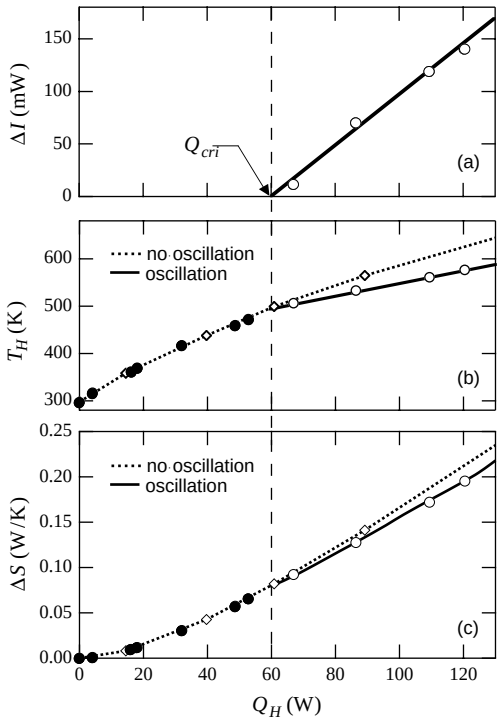

Fig. 3

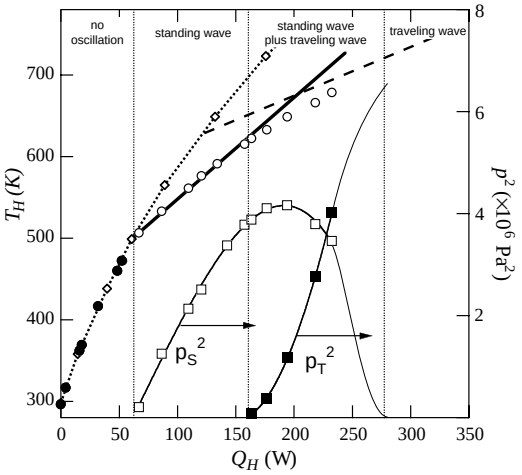

Fig. 4

Fig. 3 – The variation of ΔI (a), $T_{\rm H}$ (b) and ΔS (c) as a function of $Q_{\rm H}$, when the gas oscillations are absent (solid circles) and present (open circles). Open diamonds in (b) are measured when the gas oscillations are suppressed and those in (c) represent the corresponding variation of ΔS. The vertical dashed line represents the critical heat flow $Q_{\rm cri} = 60\,{\rm W}$.

Fig. 4 – $Q_{\rm H}$-dependence of $T_{\rm H}$ (solid and open circles) in the present engine. The variation of the square of pressure amplitudes for standing- (open squares) and traveling- (solid squares) wave modes in the present engine is also shown as a function of $Q_{\rm H}$. Vertical dotted lines represent boundaries among the no-oscillation, standing-wave mode, quasiperiodic states and traveling-wave mode. The dotted line with open diamonds represents the variation in $T_{\rm H}$ when the gas oscillations are absent, and the dashed line is measured in a looped-tube engine without a resonator in fig. 1(b).

of $T_{\rm H}$, measured when the oscillations are suppressed, is also shown in fig. 3(b) by a dotted curve. In the nonoscillating region $0 \le Q_{\rm H} < Q_{\rm cri}$, $T_{\rm H}$ increases monotonically from $T_{\rm C}$ with increasing $Q_{\rm H}$, while ΔI remains zero. An increase in the entropy flow ΔS in the absence of oscillations is simply given by eq. (2). As shown by the dotted curve in fig. 3(c), ΔS is zero only in the equilibrium state with $Q_{\rm H} = 0$, and increases with increasing $Q_{\rm H}$. The positive ΔS can be attributed to the irreversible thermal conduction through the solid walls and the working fluid.

In the region $Q_{\rm H} \ge Q_{\rm cri}$, the self-sustained oscillation of the standing-wave mode is induced. This is evidenced by a finite ΔI above $Q_{\rm cri}$. The output power ΔI begins to increase linearly from $Q_{\rm cri}$ with increasing $Q_{\rm H}$, while $T_{\rm H}$ *vs.* $Q_{\rm H}$ reduces its slope discontinuously at $Q_{\rm cri}$. Consequently, $T_{\rm H}$ becomes smaller than that without oscillations. We deduced an increase in the entropy flow ΔS in the presence of oscillations by inserting the data above into

eq. (3), and plotted it in fig. 3(c) by open circles with a thick full curve. Notably, ΔS in the presence of the gas oscillations lies consistently below the dotted line above $Q_{\rm cri}$. This means that the value of ΔS is definitely lowered by the emergence of the standing-wave mode oscillation in the range $Q_{\rm H}$ above $Q_{\rm cri}$. It is clear from eq. (3) that the reduction in ΔS is caused by both the production of ΔI and the reduction in $T_{\rm H}$, but the latter turned out to reduce ΔS much more than the former. Indeed, ΔI and $T_{\rm H}$ contributions were 3 and 97% to the total reduction in ΔS, respectively, when $Q_{\rm H} = 86\,{\rm W}$. This enables us to determine the ΔS-$Q_{\rm H}$ relation only from the $T_{\rm H}$-$Q_{\rm H}$ relation without measuring ΔI in the present engine.

On the basis of the experimental findings above, we measured the $T_{\rm H}$ *vs.* $Q_{\rm H}$ relation up to 230 W to determine the ΔS-$Q_{\rm H}$ relation in the further higher $Q_{\rm H}$ region. As shown by the circles in fig. 4, $T_{\rm H}$ in the present engine increases linearly above $Q_{\rm cri}$ ($= 60\,{\rm W}$), but the slope of $T_{\rm H}$ becomes small, when $Q_{\rm H}$ exceeds 160 W. This is brought about by a change in the oscillating mode from the standing to the quasiperiodic state consisting of both the standing- and traveling-wave modes. Here the traveling-wave mode refers to the acoustic traveling wave with a fundamental frequency of 273 Hz running around the loop in the direction from $T_{\rm C}$ to $T_{\rm H}$ through the stack. Only the traveling-wave mode is excited in a looped tube engine [10]. The dashed line in fig. 4 represents the $T_{\rm H}$-$Q_{\rm H}$ curve measured for the looped-tube engine after removing the resonator from the present assembly in fig. 1. Obviously, the dashed line due to the traveling-wave mode lies above the solid line due to the standing-wave mode above $Q_{\rm cri}$, but crosses with it at about 200 W. Since $T_{\rm H}$ *vs.* $Q_{\rm H}$ behavior directly reflects the ΔS *vs.* $Q_{\rm H}$ relation, we conclude that the superposition of the traveling-wave mode above 160 W contributes to a further reduction in ΔS, in comparison with that due to the nonoscillating mode and that due to the standing-wave mode.

As is presented by three different lines in fig. 4, there definitely exist three different modes in the present engine, nonoscillating-, standing- and traveling-wave modes. Indeed, $\Delta S > 0$ holds in any of these modes, but the present engine clearly demonstrates successive mode transitions with increasing $Q_{\rm H}$, in such a way that the mode with the lowest ΔS is always selected. The argument above leads us to propose a thermodynamical mode selection rule: *a mode having a minimum increase in entropy flow is selected among all permissible modes.* In other words, the mode transitions in the present engine occurs because of the crossing of ΔS inherent in each mode on a ΔS-$Q_{\rm H}$ diagram.

In the quasiperiodic state of the present engine, the power spectra of the measured pressure oscillations are found to consist of sharp peaks at frequencies given by a linear combination of the fundamental frequencies of the standing- and the traveling-wave modes, as well as their higher harmonics. Incorporated in fig. 4 is the square of the pressure amplitudes $p_{\rm S}^2$ and $p_{\rm T}^2$ at fundamental frequencies for the standing- and traveling-wave modes measured at $x = 0.11$. As can be seen, $p_{\rm S}^2$ increases linearly in the region above $Q_{\rm cri}$, but, in the quasiperiodic states, $p_{\rm S}^2$ decreases after showing a maximum. On the other hand, $p_{\rm T}^2$ increases quickly above $Q_{\rm H} = 160\,{\rm W}$. A smooth variation of $p_{\rm S}^2$ and $p_{\rm T}^2$ with $Q_{\rm H}$ is responsible for a continuous change in the slope of $T_{\rm H}$, which is in contrast to the discontinuous one in $T_{\rm H}$ observed when the standing-wave mode emerges. We believe that a fraction of these two modes is determined so as to minimize ΔS through nonlinear interactions between them in accordance with the mode selection rule. Further increase in $Q_{\rm H}$ would result in the transition from the quasiperiodic states to the traveling-wave mode, where $p_{\rm S}^2$ decreases to zero and $T_{\rm H}$ eventually approaches the dashed line in fig. 4. Indeed, we have observed a complete transition to the traveling-wave mode in a similar, but smaller thermoacoustic engine in spite of the limited power up to 230 W.

In conclusion, we built a thermoacoustic engine consisting of the looped tube and the resonator, and observed successive transitions from the standing- to traveling-wave modes

through the quasiperiodic state with increasing nonequilibrium parameter Q_{H}. It was found that the emergence of the spontaneous gas oscillations and the transition to the traveling-wave mode can be well understood in terms of a minimum increase in entropy flow through the stack. The mode selection rule that we have proposed would also provide thermodynamical interpretation for the transition sequences observed in other nonlinear dissipative systems.

REFERENCES

[1] Nicolis G. and Prigogine I., *Self-Organization in Nonequilibrium Systems* (John Wiley & Sons, New York) 1977.

[2] Wheatley J., Hofler T., Swift G. W. and Migliori A., *Phys. Rev. Lett.*, **50** (1983) 499; *J. Acoust. Soc. Am.*, **74** (1983) 153; *Am. J. Phys.*, **53** (1985) 147.

[3] Swift G. W., *Phys. Today*, **48** (1995) 22; *J. Acoust. Soc. Am.*, **84** (1988) 1145.

[4] Tominaga A., *Cryogenics*, **35** (1995) 427.

[5] Work and heat flows due to the oscillating gas are defined as $I = A\overline{P \cdot U}$ and $Q = T_{\mathrm{m}}S$; a bar represents a time average; A, P and U are, respectively, the cross-sectional area of the fluid passage, cross-sectional mean velocity, and pressure for the oscillating gas; T_{m} and S are mean temperature, and entropy flow defined as $S = A\rho_{\mathrm{m}}\langle\overline{s \cdot V}\rangle$, where the angular bracket represents a radial average; ρ_{m}, s and V are, respectively, the mean mass density, entropy per unit mass and axial velocity for the oscillating gas.

[6] Atchley A. A., *J. Acoust. Soc. Am.*, **95** (1994) 1661.

[7] Yazaki T., Tominaga A. and Naramara Y., *J. Low Temp. Phys.*, **41** (1980) 45.

[8] Yazaki T. and Tominaga A., *Proc. R. Soc. London, Ser. A*, **454** (1998) 2113.

[9] Backhaus S. and Swift G. W., *Nature*, **399** (1999) 335.

[10] Yazaki T., Iwata A., Maekawa T. and Tominaga A., *Phys. Rev. Lett.*, **81** (1998) 3128.

[11] Biwa T., Ueda Y., Yazaki T. and Mizutani U., in *Proceedings of the 17th International Congress on Acoustics, Part A, Rome, 2001.*

[12] Heslot F., Castaing B. and Libchaber A., *Phys. Rev. A*, **36** (1987) 5870.

[13] Krishnamurti J. R., *Fluid Mech.*, **60** (1973) 285.

[14] Tominaga A., in *Proceedings of the 17th International Congress on Acoustics, Part A, Rome, 2001.*

[15] We found the setup in which the oscillations were not induced with our maximum Q_{H}. A T_{H}-Q_{H} relation was also measured for this setup, which is shown in figs. 3 and 4.

[16] The axial distribution of the pressure amplitude for the standing-wave mode in the present engine shows its maxima at $x = 0$ and at the closed end of the resonator, while that along the looped tube is symmetrical with respect to $x = 0.5$, the connecting point of the looped tube and the resonator.